Effect of self-organization in polymer/fullerene bulk heterojunctions on solar cell performance

Vishal Shrotriya, Yan Yao, Gang Li, and Yang Yang[a)]
Department of Materials Science and Engineering, University of California, Los Angeles, Los Angeles, California 90095

(Received 20 January 2006; accepted 20 June 2006; published online 9 August 2006)

The authors investigate the effect of self-organization by controlling the growth rate on the performance of polymer/fullerene bulk-heterojunction solar cells. The effect of growth rate on the morphology of the active layer is studied by atomic force microscopy technique. The electrical characterization by dark current and photocurrent measurements is performed. The hole mobility in the polymer increases by about two orders in magnitude and the carrier transport becomes highly balanced. Increased exciton generation rate, more efficient electron-hole pair dissociation, higher carrier mobility, and balanced carrier transport in the active layer explain the enhancement in the short-circuit current and fill factor. © *2006 American Institute of Physics*.
[DOI: 10.1063/1.2335377]

In the last decade, polymer photovoltaic (PV) cells have emerged as a promising source of nonconservative, renewable, and truly clean energy.[1,2] Highly efficient solar cells based on bulk-heterojunction (BH) poly (3–hexylthipphene) (P3HT) with[6,6]-phenyl-C_{61}-butyric acid methyl ester (PCBM) have been demonstrated.[3–5] Recently, we reported very efficient plastic solar cells based on P3HT/PCBM where controlling the growth rate of the active layer resulted in a significant enhancement in device efficiency.[6] In this letter, we investigate in detail the mechanisms behind efficiency improvement in P3HT/PCBM devices. The effect of self-organization by slow growth on the active layer morphology is examined by atomic force microscope (AFM) technique. The transport properties of the materials are studied by fitting the current-voltage (J-V) characteristics measured under dark to the space-charge limited current (SCLC) model.[7,8] Finally, the photocurrent behavior of PV devices under reverse bias is examined based on Onsager's theory[9] of ion-pair dissociation in weak electrolytes. The effect of growth rate on the dissociation efficiency of electron-hole (e-h) pair under short-circuit conditions is examined, and its effect on the device performance is discussed.

The device fabrication procedure for regular P3HT/PCBM devices is described elsewhere.[6] To make hole-only devices, Ca was replaced with higher work function MoO_3 as the top contact. A thin layer of MoO_3 was thermally evaporated on top of the active layer and capped with 50 nm of Al. For the electron-only devices, polyethylenedioxythiophene-:polystyrenesulfonate (PEDOT:PSS) layer was replaced with a thin layer of Cs_2CO_3 spin coated from solution in 2-ethoxyethanol. Testing was done in N_2 under simulated AM 1.5G irradiation (100 mW/cm^2) using xenon-lamp based solar simulator (Oriel 96000 150W Solar Simulator). Digital Instruments multimode scanning probe microscope was used to obtain the AFM images. Figure 1 shows the AFM phase images for P3HT/PCBM films that are grown at different rates. The images are obtained in tapping mode for a 1×1 μm^2 surface area. The phase image of the fast grown film [Fig. 1(a)] shows coarse chainlike features running across the surface. These features are assigned to the domains of pure P3HT crystallites each of which contains several polymer chains tightly packed. The region between these features consists of either P3HT/PCBM mixed domains or pure PCBM clusters. PCBM molecules suppress the formation of P3HT crystallites in the fast grown films and most of the film consists of mixed domains which are amorphous in nature. For the slow grown film, however, the crystalline domains of pure P3HT chains are denser and are distributed more uniformly throughout the film [Fig. 1(b)]. The separation distance between surface features in slow grown film (~28 nm) is smaller than that in fast grown film (~55 nm). The crystallite size estimated from AFM phase images

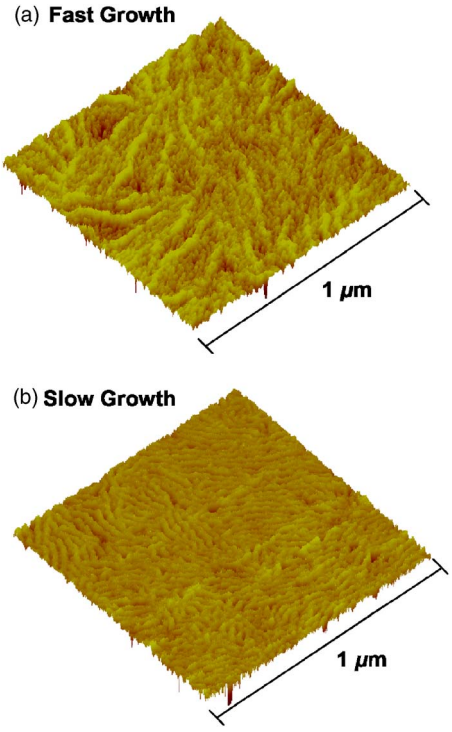

FIG. 1. (Color online) Effect of growth rate induced self-organization on the morphology of the active layer. AFM phase image of (a) fast grown and (b) slow grown polymer/fullerene blend films for a 1×1 μm^2 surface area.

[a)]Electronic mail: yangy@ucla.edu

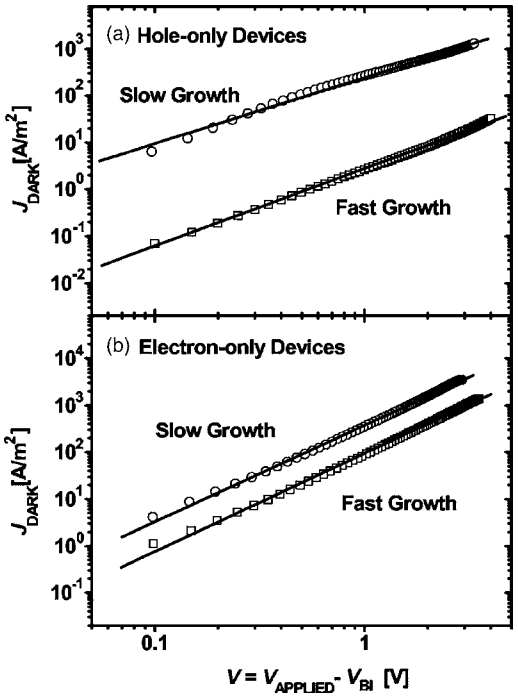

FIG. 2. Measured *J-V* characteristics under dark for (a) hole-only and (b) electron-only PV devices consisting of P3HT/PCBM active layer grown at fast and slow rates. The solid lines represent the fit to the experimental data using SCLC model. The bias is corrected for built-in potential (V_{bi}), arising from difference in the work function of the contacts, so that $V=V_{applied}-V_{bi}$. V_{bi} values are 0.1 V for both hole- and electron-only devices.

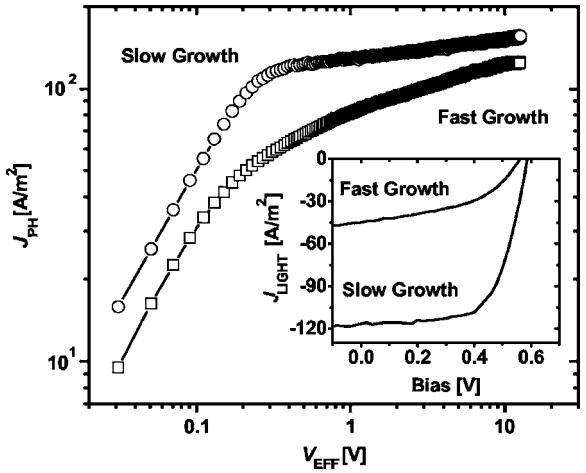

FIG. 3. Measured photocurrent as a function of effective applied bias for PV devices with fast and slow grown active layers. The *J-V* characteristics under illumination (130 mW/cm^2, simulated AM 1.5G) for two PV devices with different active layer growth rates are shown in the inset.

matches the results from x-ray diffraction data on similar films[10,11] where mean crystallite size estimated from Scherrer's equation is 10–50 nm. The reduced crystallite size and intercrystallite spacing are believed to be the result of higher ordering.

In polymer BHJ solar cells an important factor in determining external quantum efficiency is the carrier transport in the active layer. Various techniques, including time-of-flight (TOF) measurement,[12,13] field effect transistor characteristics,[14] photoinduced charge extraction in linearly increasing voltage technique,[15] and *J-V* curve fitting using SCLC model,[16,17] have been used to experimentally determine the electron and hole mobilities. We recently reported electron and hole mobility values, measured by TOF technique for slow grown P3HT/PCBM films, of $\mu_e \sim 8\times10^{-9}$ and $\mu_h \sim 5\times10^{-9}$ m^2 V^{-1} s^{-1} resulting in highly balanced carrier transport ($\mu_e/\mu_h \sim 1.5$). However, in the TOF measurements, a much thicker film was used, about five times thicker than the actual device. To make a realistic estimate of the carrier mobilities in the blend film and accurate comparison of electron and hole mobilities, it is important to perform the measurements on the same device configuration as the actual device. The electron and hole mobilities can be measured precisely by fitting the dark *J-V* curves for single carrier devices to SCLC model at low voltages, where the current is given by $J=9\varepsilon_0\varepsilon_r\mu V^2/8L^3$ (Ref. 11), where $\varepsilon_0\varepsilon_r$ is the permittivity of the polymer, μ is the carrier mobility, and L is the device thickness. Figure 2 shows the log *J*-log *V* curves for (a) hole-only and (b) electron-only devices where the active layer of P3HT/PCBM was obtained by slow and fast growth. The applied bias voltage is corrected for the built-in potential so that $V=V_{applied}-V_{bi}$. Molybdenum oxide (MoO_3), with work function (Φ)=5.3 eV as measured in our laboratory by ultraviolet photoelectron spectroscopy (UPS), is a good hole injection contact for P3HT/PCBM.[18] A large energy barrier between lowest unoccupied molecular orbital of PCBM and Φ of MoO_3 ($\Delta E \sim 1.6$ eV) suppresses electron injection from the top electrode rendering the device hole-only characteristics. Cesium carbonate (Cs_2CO_3) has been used as an efficient electron-injection layer for organic electroluminescent devices.[19] The work function of Cs_2CO_3 was found to be ~2.9 eV by UPS measurements conducted in our laboratory. Therefore, it can replace polyethylenedioxythiophene:polystyrenesulfonate (PEDOT:PSS) as the anodic buffer layer to make electron-only devices. For the fast grown films, the mobilities are $\mu_e \sim 6.5\times10^{-8}$ and $\mu_h \sim 1.9\times10^{-9}$ m^2 V^{-1} s^{-1}. For slow grown film, the electron mobility increases by four times to 2.6×10^{-7} m^2 V^{-1} s^{-1}, but the hole mobility increases by about two orders of magnitude to 1.7×10^{-7} m^2 V^{-1} s^{-1}. The ratio of electron to hole mobility is therefore ~1.5 times, which is similar to the observation from TOF measurements. A relatively small increase in μ_e (by four times) upon slow growth is understandable because the slow growth of the blend results primarily in an increased ordering in the polymer chains which will significantly effect the hole mobility, whereas it will have small effect on the electron mobility in PCBM. An increase of two orders in magnitude in μ_h upon slow growth further supports this argument.

To study the effect of growth rate of the active layer on the photocurrent generation in the device, we measured the *J-V* characteristics in reverse bias under 130 mW/cm^2 simulated AM 1.5G conditions. The devices were biased in a sweep from +0.8 to −15.0 V. Figure 3 shows the photocurrent (J_{ph}) as a function of the effective applied bias $V_{eff}=V_0-V$, where V is the applied bias. J_{ph} is the obtained by correcting the current under illumination for the dark current, i.e., $J_{ph}=J_{light}-J_{dark}$, and V_0 is the bias where $J_{light}=J_{dark}$. Also shown in the inset of Fig. 3 are the *J-V* characteristics under illumination for the fast and slow grown films. In the low effective field region ($V_{eff}<0.1$ V), the photocurrent increases linearly with voltage for both types of devices. Such behavior has been reported earlier by Mihailetchi *et al.*[17,20] At large reverse bias ($V_{eff}>10$ V), J_{ph} saturates for both devices with saturation photocurrent (J_{sat}) of ~125 A/m^2 for

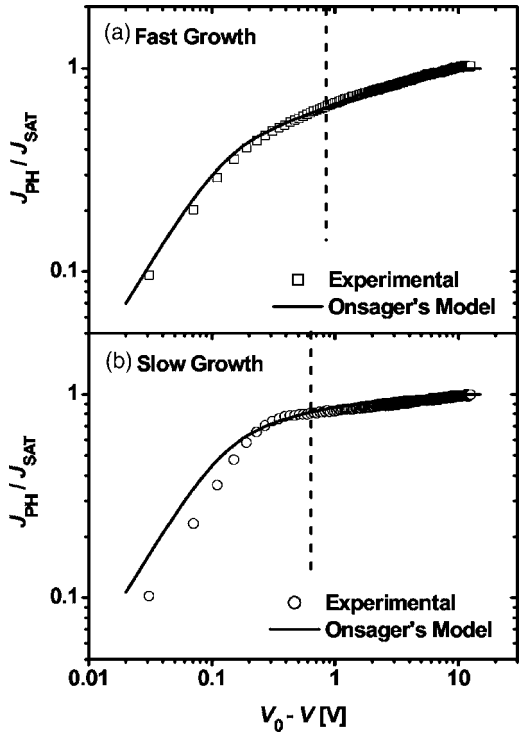

FIG. 4. Measured (open symbols) and calculated (solid curves) normalized photocurrent as a function of effective applied bias for (a) fast and (b) slow grown films. The solid curves represent the J_{ph}/J_{sat} values calculated from Onsager's model.

the fast and $\sim 155\ \mathrm{A/m^2}$ for the slow grown films. The maximum generation rates (G_{max}) (given as $J_{sat}=eG_{max}L$) are 3.5×10^{27} and $4.4\times10^{27}\ \mathrm{m^{-3}\ s^{-1}}$ for the fast and slow grown films (thickness $L=220$ nm). Upon changing the growth rate of the film from fast to slow, the *e-h* pair generation in the film increases by about 26%. This increase is attributed to the increased absorption in the active layer when the film is grown slowly.[6]

To compare the photocurrent behavior, we have plotted the normalized photocurrent (J_{ph}/J_{sat}) for the fast and slow grown films in Figs. 4(a) and 4(b). The short-circuit operation point ($V_{eff}=V_0$) for both types of devices is marked by a dashed line parallel to the *y* axis in the figures. At any given electric field and temperature, only a certain fraction of photogenerated *e-h* pairs will dissociate into free carriers with dissociation probability $P(E,T)$. This gives the generation rate at any given electric field and temperature as $G(E,T)=G_{max}P(E,T)$ and the photocurrent as $J_{ph}=eG_{max}P(E,T)L$.[20] Onsager's theory[9] of ion-pair dissociation in weak electrolytes, modified by Braun,[21] has been used in the past to describe the J_{ph}-V behavior in solar cells.[20] First we examine the J_{ph}-V behavior for the fast grown film. From the Onsager's model, an exact fit to the experimental data can be obtained in the complete bias range (solid curve). At the short-circuit condition ($V=0$ or $V_{eff}=V_0$), only 57% of the total photogenerated *e-h* pairs dissociate into free carriers, which further reduces to 41% at the maximum power output point ($V=0.4$ V). This suggests that more than half of the *e-h* pairs that are generated after photoinduced charge transfer are lost due to recombination in the active layer before they can be separated into free carriers. On the other hand, the photocurrent behavior of the slow grown film shows some very interesting features. At the short-circuit condition, the *e-h* pair dissociation efficiency is more than 80%, which is probably the highest value observed in a polymer BHJ device so far. At the maximum power output bias, the efficiency is still around 70%. Such high dissociation efficiency numbers clearly demonstrate the effect of self-organization induced ordering in the blend films. It is also interesting to note the steeper field dependence of generation rate in the low range to midrange fields for the slow grown film. The J_{ph}/J_{sat} curve shows saturation behavior at very low bias and does not increase much after this point. This behavior is very similar to the observation made by Goliber and Perlstein[22] where they used a delta distribution function, instead of a Gaussian, for the charge-transfer (CT) radii.

Based on the mobility and photocurrent measurements discussed above, we conclude that the effect of growth rate on the performance is understood to be threefold—higher exciton generation, higher dissociation efficiency of *e-h* pair (up to 80%), and increase in hole mobility by roughly two orders of magnitude which coupled with a fourfold increase in the electron mobility results in a highly balanced charge transport.

The authors thank Douglas Sievers for several valuable discussions. This research work is supported by the Office of Naval Research (Grant No. N00014-04-1-0434, Program Manager: Paul Armistead).

[1] C. J. Brabec, V. Dyakonov, J. Parisi, and N. S. Sariciftci, *Organic Photovoltaics: Concepts and Realization* (Springer, Heidelberg, 2003).
[2] S.-S. Sun and N. S. Sariciftci, *Organic Photovoltaics: Mechanism, Materials, and Devices (Optical Engineering)* (CRC, Boca Raton, FL, 2005).
[3] G. Li, V. Shrotriya, Y. Yao, and Y. Yang, J. Appl. Phys. **98**, 043704 (2005).
[4] W. Ma, C. Yang, X. Gong, K. Lee, and A. J. Heeger, Adv. Funct. Mater. **15**, 1617 (2005).
[5] M. Reyes-Reyes, K. Kim, and D. L. Carroll, Appl. Phys. Lett. **87**, 083506 (2005).
[6] G. Li, V. Shrotriya, J. Huang, Y. Yao, T. Moriarty, K. Emery, and Y. Yang, Nat. Mater. **4**, 864 (2005).
[7] M. A. Lampart and P. Mark, *Current Injection in Solids* (Academic, New York, 1970).
[8] P. W. M. Blom, M. J. M. de Jong, and M. G. van Munster, Phys. Rev. B **55**, R656 (1997).
[9] L. Onsager, J. Chem. Phys. **2**, 599 (1934).
[10] T. Erb, U. Zhokhavets, G. Gobsch, S. Raleva, B. Stühn, P. Schilinsky, C. Waldauf, and C. J. Brabec, Adv. Funct. Mater. **15**, 1193 (2005).
[11] V. Shrotriya and A. Noori (unpublished).
[12] S. A. Choulis, J. Nelson, Y. Kim, D. Popalavsky, T. Kreouzis, J. R. Durant, and D. D. C. Bradley, Appl. Phys. Lett. **83**, 3812 (2003).
[13] J. Huang, G. Li, and Y. Yang, Appl. Phys. Lett. **87**, 112105 (2005).
[14] W. Geens, T. Martens, J. Poortmans, T. Aernouts, J. Manca, L. Lutsen, P. Heremans, S. Borghs, R. Mertens, and D. Vanderzande, Thin Solid Films **451–452**, 498 (2004).
[15] A. J. Mozer, N. S. Sariciftci, L. Lutsen, D. Vanderzande, R. Österbacka, M. Westerling, and G. Juška, Appl. Phys. Lett. **86**, 112104 (2005).
[16] C. Melzer, E. J. Koop, V. D. Mihailetchi, and P. W. M. Blom, Adv. Funct. Mater. **14**, 865 (2004).
[17] V. D. Mihailetchi, L. J. A. Koster, P. W. M. Blom, C. Melzer, B. de Boer, J. K. J. van Duren, and R. A. J. Janssen, Adv. Funct. Mater. **15**, 795 (2005).
[18] V. Shrotriya, G. Li, Y. Yao, C.-W. Chu, and Y. Yang, Appl. Phys. Lett. **88**, 073508 (2006).
[19] J. Huang, G. Li, E. Wu, Q. Xu, and Y. Yang, Adv. Mater. (Weinheim, Ger.) **18**, 114 (2006).
[20] V. D. Mihailetchi, L. J. A. Koster, J. C. Hummelen, and P. W. M. Blom, Phys. Rev. Lett. **93**, 216601 (2004).
[21] C. L. Braun, J. Chem. Phys. **80**, 4157 (1984).
[22] T. E. Goliber and J. H. Perlstein, J. Chem. Phys. **80**, 4162 (1984).